DOI: 10.1002/cbic.200900024

# Design of Triazole-Tethered Glycoclusters Exhibiting Three Different Spatial Arrangements and Comparative Study of their Affinities towards PA-IL and RCA 120 by Using a DNA-Based Glycoarray

Lisa Moni,[a] Gwladys Pourceau,[b] Jing Zhang,[c] Albert Meyer,[b] Sébastien Vidal,[d] Eliane Souteyrand,[c] Alessandro Dondoni,[a] François Morvan,[b] Yann Chevolot,[c] Jean-Jacques Vasseur,*[b] and Alberto Marra*[a]

Interactions between proteins and carbohydrates are involved in a large number of crucial biological events. Many efforts have been devoted to the design and synthesis of unnatural saccharides displaying high affinities towards targeted lectins. Among others, glycoside clusters have proven to be valuable tools for these recognition studies. However, the spatial arrangements of the sugar residues are a key issue in the design of high-affinity glycoclusters. Here, the affinities of linear and antenna- and calixarene-based galactoside clusters against two lectins, derived from *Pseudomonas aeruginosa* and *Ricinus communis*, have been compared by means of glycoarrays.

## Introduction

Many key physiological and pathological events occur through interactions between carbohydrate and sugar-binding proteins called lectins. Host–pathogen recognition offers many examples of such interactions. The first step of influenza virus infection, for example, involves the viral-hemagglutinin-mediated adhesion of the virion to sialic acid residues present on the surfaces of endothelial cells. A similar approach is exploited by bacteria and parasites.

Therefore, understanding of the structure–function relationships of this molecular recognition process may provide access to innovative therapeutic strategies. Nevertheless, because natural carbohydrate–lectin interactions are usually weak, glycochemists have devoted much effort to the design of high-affinity artificial ligands, including glycosides bearing hydrophobic aglycons[1] and, more recently, glycoclusters,[2] to take advantage of the so-called cluster effect.[3–5] It is worth noting that in the case of glycoclusters the affinity is not only related to the multivalency.[6] In fact, different authors have demonstrated the importance of the spatial distributions of the glycoside residues for obtainment of high affinities.[7]

Calix[4]arenes can be synthesized in various blocked conformations, thus providing a series of well-defined geometries for the display of sugar ligands. A recent study demonstrated that *N*-glycosylated calix[*n*]arenes of variable valencies and geometries are capable of distinguishing among lectins of a family.[8]

Here we report the synthesis of *C*-glycosylated calix[4]arenes in which four galactose residues are linked through alkyl triazole tethers to the upper rim of the macrocycle cavity whereas an azido group is present on the opposite side. Next, the calixsugars were grafted through copper-mediated azide–alkyne cycloaddition (CuAAC) onto mono- or dipropargyloxymethylpropanediol moieties, allowing the synthesis of oligonucleotides bearing one or two calixarene glycoclusters, respectively. Finally, their affinities towards the lectins PA-IL[9] and RCA 120, galactose-specific lectins from *Pseudomonas aeruginosa* and *Ricinus communis*, respectively, were compared to those displayed by linear and antenna-type glycoclusters.[10,11] The evaluation of the affinity of each glycomimic was performed on a DNA-based glycoarray platform as previously described[12] by direct fluorescence scanning and by determination of its $IC_{50}$ value.[13]

[a] *Dr. L. Moni, Prof. Dr. A. Dondoni, Prof. Dr. A. Marra*
*Dipartimento di Chimica, Laboratorio di Chimica Organica*
*Università di Ferrara, Via L. Borsari 46, 44100, Ferrara (Italy)*
*Fax: (+39) 0532-455167*
*E-mail: mra@unife.it*

[b] *G. Pourceau, A. Meyer, Dr. F. Morvan, Dr. J.-J. Vasseur*
*Institut des Biomolecules Max Mousseron, Département des Analogues et Constituants des Acides Nucléiques, UMR 5247 CNRS*
*Université Montpellier 1, Université Montpellier 2*
*Place E. Bataillon, CC1704, 34095 Montpellier Cedex 5 (France)*
*Fax: (+33) 467-042-029*
*E-mail: vasseur@univ-montp2.fr*

[c] *J. Zhang, Dr. E. Souteyrand, Dr. Y. Chevolot*
*Institut des Nanotechnologies de Lyon, UMR 5270 CNRS*
*Ecole Centrale de Lyon, Université Claude Bernard Lyon 1*
*Equipe Chimie et Nanobiotechnologies*
*36 Avenue Guy-de-Collongue, 69134 Ecully (France)*

[d] *Dr. S. Vidal*
*Institut de Chimie et Biochimie Moléculaires et Supramoléculaires*
*UMR 5246 CNRS, Université Lyon Claude Bernard 1-CPE*
*Laboratoire de Chimie Organique 2-Glycochimie*
*43 Boulevard du 11 Novembre 1918, 69622 Villeurbanne (France)*

*Supporting information for this article is available on the WWW under http://dx.doi.org/10.1002/cbic.200900024.*

  

## Results and Discussion

### Synthesis of *C*-galactosyl calix[4]arene clusters

We designed the calix[4]arene-based glycoclusters **1** and **2**, each functionalized with a single azido group, with the aim of introducing these multiglycosylated molecules into oligonucleotides by means of copper-catalyzed azide–alkyne cycloadditions (click chemistry).[14] The calix[4]arenes were chosen as platforms because they can be easily derivatized at both the upper (wide) and lower (narrow) rims and they are endowed with well-organized three-dimensional architectures.[15] Of the four possible conformations (cone, partial cone, 1,2-alternate, 1,3-alternate) adopted by calix[4]arenes, the cone structure allows a spatially close arrangement of the four sugar ligands on one side of the macrocycle.

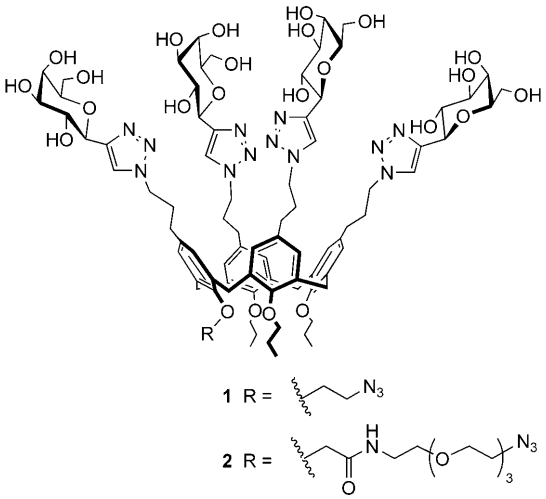


The synthesis of densely substituted calix[4]arenes **1** and **2** is briefly described. The key intermediate **7** was first targeted, through standard calixarene chemistry from the known[16] tetraallyl-calix[4]arene **3** (Scheme 1). Compound **7** featured four azidopropyl groups at its upper rim and only one free hydroxy group at its lower rim, whereas the other three hydroxy groups were protected as *O*-propyl ethers to insure a blocked cone conformation of the macrocycle. Unfortunately though, the regioselective, direct protection of three phenolic hydroxy groups in a calix[4]arene derivative is not a trivial task. In fact, the synthesis of lower-rim dialkylated[17] and tetraalkylated[18] calix[4]arenes in the cone conformation is a straightforward transformation, whereas the preparation of the corresponding trialkyl ethers is troublesome and often requires multistep methods.[19,20] One well-known procedure[18,21] for the synthesis of tri-*O*-alkylated calix[4]arenes involves the treatment of a tetrahydroxy derivative with an excess of an alkyl halide in the presence of BaO and $Ba(OH)_2$. However, when the tetraallylcalix[4]arene **3** was subjected to these reaction conditions, both the di- and the tripropyl ethers were formed in low yields (about 25% each). The target tetraazidated calixarene **7** was thus prepared from the starting compound **3** by use of an alternative strategy to differentiate one of the four hydroxy groups at the lower rim. Taking advantage of our previous studies on the synthesis of calix[4]arene-based glycoclusters,[22–25] we monoglycosylated **3** by treatment with commercially available α-D-mannofuranose diacetonide (**4**, 1.1 equiv) under Mitsunobu conditions,[22] and the three residual hydroxy groups were then protected as *O*-propyl ethers to give compound **5** in 80% isolated yield (two steps). The first step of this new procedure afforded a monoprotected calix[4]arene in a yield similar to or even better than those registered by previous methods based on the use of NaOMe[20] (70–80%), LiOH[26] (73–85%), $K_2CO_3$[27] (37–88%), CsF[27] (60–85%), or $(Bu_3Sn)_2O$[28] (47–80%) and very simple alkyl halides.[29]

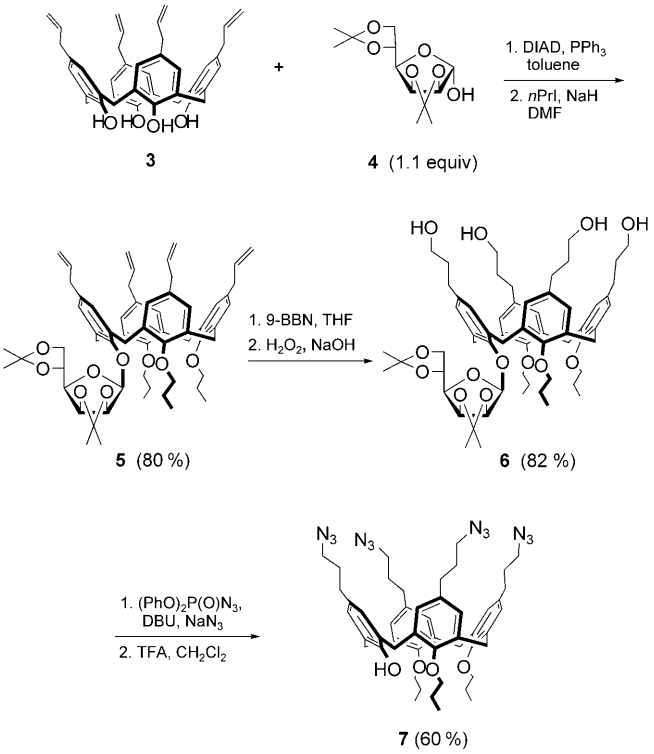


**Scheme 1.** Preparation of the key intermediate (**7**) bearing four azido functions and a single hydroxy group.

With compound **5** to hand, with all hydroxy groups suitably protected, the multiple hydroboration-oxidation of the four allyl groups at the upper rim was readily carried out to give the tetrol **6**. Subsequent transformation by azidation with diphenylphosphoryl azide and sodium azide, followed by removal of the mannofuranose fragment by acidic hydrolysis, afforded the tetraazide **7**.

In order to obtain the glycocluster **1**, which features the azido group in close proximity to the macrocycle cavity, the free hydroxy group of **7** was alkylated with the short *N*-Boc ethylamino chain to give **8** (Scheme 2). The adoption of the fixed-cone conformation in the calix[4]arene macrocycle by **8** was supported by the presence of signals for the equatorial and axial protons of the methylene bridges as doublets at about 3.1 and 4.3 ppm, respectively, in its $^1H$ NMR spectrum. Click chemistry was then performed on the tetraazide **8** as

  

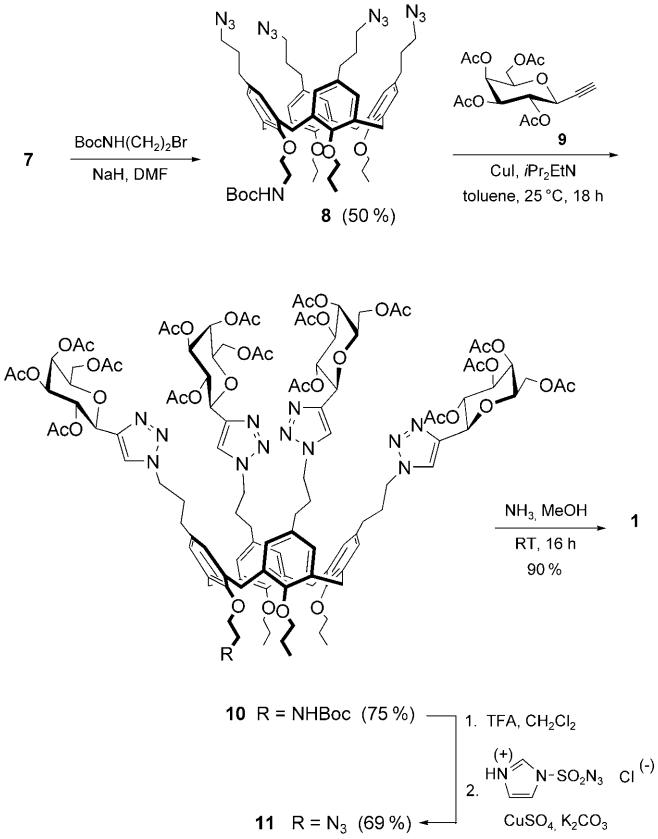


**Scheme 2.** Synthesis of the glycocluster **1** by copper(I) mediated azide–alkyne cycloaddition and diazo-transfer reaction.

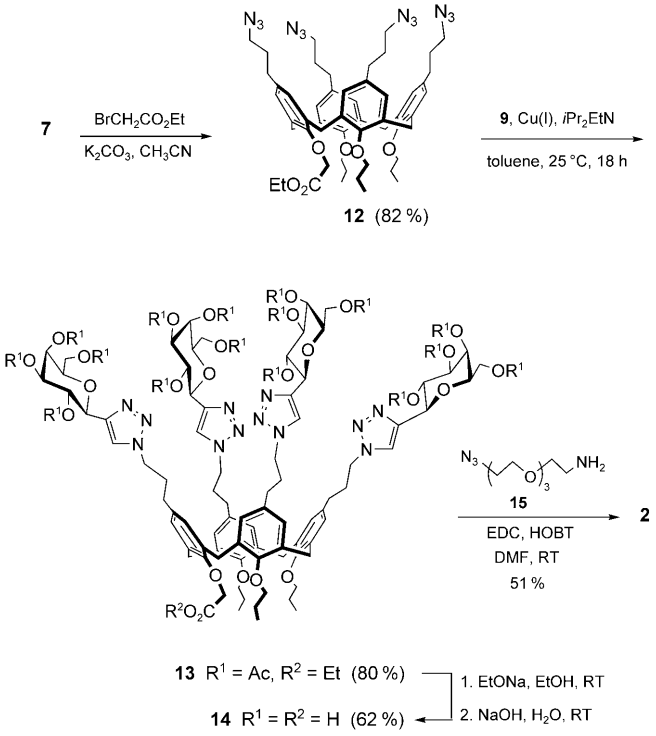


**Scheme 3.** Synthesis of the glycocluster **2** by CuAAC and treatment with long-chain aminoazide **15**.

described in earlier reports from our laboratory.[24,25] Accordingly, **8** was allowed to react with a stoichiometric amount (4.0 equiv) of the known[30] ethynyl tetra-*O*-acetyl-β-D-*C*-galactopyranoside **9** in the presence of $Cu^{I}$ and Hünig's base to give the triazole-tethered tetravalent glycosylated calix[4]arene, **10**. Quite remarkably, the four click reactions on the same substrate **8** must all have occurred quite efficiently, because compound **10** was obtained in 75% yield, corresponding to a 93% average yield for each cycloaddition reaction. This good result is very likely due to the postulated[25] complexation of a copper(I)-triazolide intermediate with the sugar alkyne, which is therefore placed in proximity to the unreacted azido groups and can readily undergo an intramolecular cycloaddition. The regioisomeric assignment of the 1,4-disubstituted 1,2,3-triazole rings was established by $^{13}C$ NMR spectroscopy as described in our earlier works.[24] Removal of the *N*-Boc group from **10** under acidic conditions, followed by a diazotransfer reaction[31] to convert the amino function into the azido group, afforded **11**. Finally, this compound was converted into the target calix[4]arene **1**, bearing carbohydrate residues at its upper rim and a single azido group at its lower rim, by treatment with ammonia in methanol.

To obtain the glycocluster **2**, featuring a long tether holding the azido group at the lower rim, the calix[4]arene derivative **7** was derivatized as the ethyl ester **12** (Scheme 3), which was subjected to the standard click reaction with the sugar alkyne **9** to give the glycocluster **13** in high yield (80%). Also in this case, the fixed cone conformation of the calix[4]arene scaffold and the 1,4-disubstitution pattern of the triazole rings were readily confirmed by $^{1}H$ and $^{13}C$ NMR analyses, respectively. Transesterification of **13**, followed by basic hydrolysis, afforded compound **14**, in which not only the ester group at the lower rim of the macrocycle but also those of the sugar residues had been removed. Finally the azido group was introduced into **14** by *N*-(3-dimethylaminopropyl)-*N'*-ethyl-carbodiimide-activated (EDC-activated) amidic coupling[32] of the free carboxylic group with the commercially available 11-azido-3,6,9-trioxaundecan-1-amine (**15**) to give the target product **2**. Compounds **1** and **2** were purified by reversed-phase column chromatography and characterized by NMR spectroscopy and MS analysis.

### Synthesis and characterization of glycocluster-oligonucleotide hybrids

The assembly of glycoclusters **1** and **2** with oligonucleotide chains was carried out in order to immobilize the resulting glycoconjugates on a microarray surface. To this end, oligonucleotides were prepared with a DNA synthesizer by standard phosphoramidite chemistry[33] on CPG (controlled pore glass) solid support, a porous borosilicate material frequently used for DNA synthesis. Two different solid-supported materials, **16**[34] and **17**[35] (Scheme 4), featuring one and two alkyne residues, respectively, were used for the synthesis of oligonucleotides **18** and **19**; each displayed the same sequence (CTG CCT CTG GGT TCA)[12] and was labeled on the 5′ end with the fluorescent dye Cy3. Treatment of **18** and **19** with concentrated aque-

  

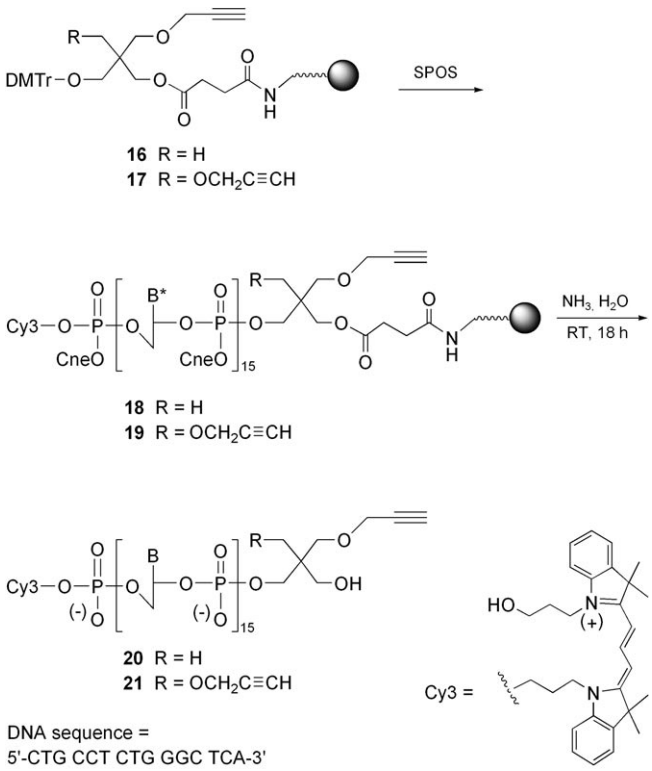


**Scheme 4.** Solid-phase oligonucleotide synthesis (SPOS) of 5′-fluorescently labeled DNA 3′-mono- or dialkynes: 1) $Cl_2CHCO_2H/CH_2Cl_2$ (2.5%), 2) phosphoramidite derivative + benzylthiotetrazole, 3) $Ac_2O$, *N*-methylimidazole, 2,6-lutidine, 4) $I_2$ ( 0.1 M), $THF/H_2O$/pyridine. The grey ball represents long-chain alkyl CPG; B* = $A^{bz}$, $C^{bz}$, $G^{ibu}$, or T and B = A, C, G or T.

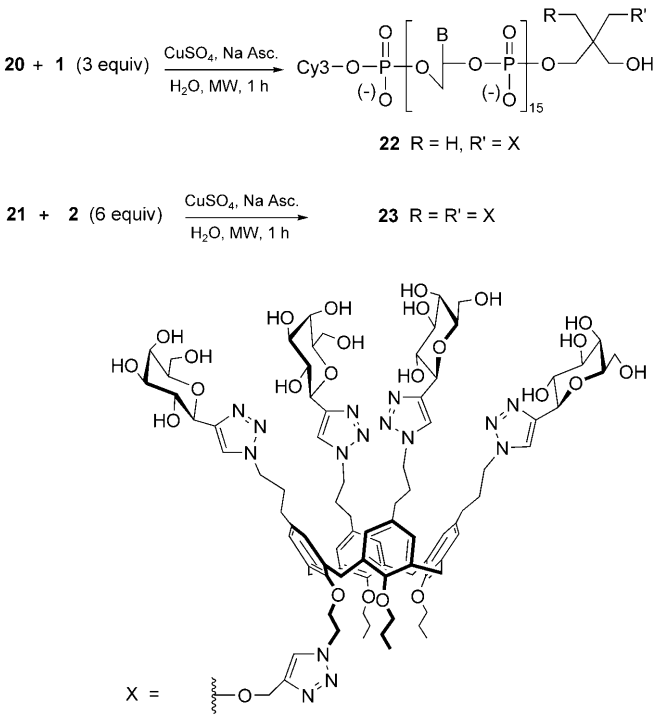


**Scheme 5.** Synthesis of the calixarene-based glycocluster oligonucleotide derivatives **22** and **23**.

ous ammonia released the oligonucleotides from the solid support and removed the protecting groups (that is, β-cyanoethyl, benzoyl, and isobutyryl) (Scheme 4). The oligonucleotides **20** and **21** were isolated, their purities were established by analytical HPLC, and they were characterized by MALDI-TOF mass spectrometry.

Because the alkyne-functionalized oligonucleotides **20** and **21** were water-soluble compounds, we set out to carry out their coupling with the azide-functionalized glycoclusters **1** and **2** (Scheme 5), respectively, in water using $CuSO_4$ and sodium ascorbate as the source of copper(I). Both reactions were performed under microwave irradiation[10] conditions in order to achieve high reaction rates and therefore to avoid some phosphodiester hydrolysis due to the presence of copper(I) ion.[36] The crude products from the click reactions were purified by preparative HPLC and characterized by MALDI-TOF mass spectrometry to give the final glycoconjugates **22** and **23**.

### Preparation of DNA-based glycoarrays to probe lectin–carbohydrate interactions

Our methodology[12] for the surface immobilization of glycoconjugates on the microarrays was as follows: 1) construction of DNA chips, 2) hybridization of the prepared glycocluster-oligonucleotide conjugates bearing the complementary DNA sequence and the fluorescent dye Cy3, and 3) addition of the fluorescently labeled lectins Cy5 or Alexa647 (Scheme 6).

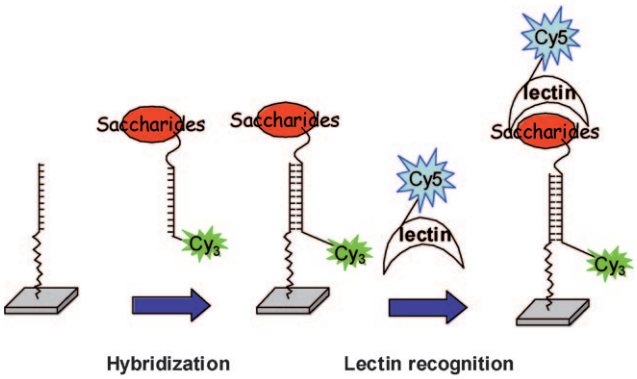


**Scheme 6.** Schematic representation of the method used to study lectin–carbohydrate interactions.

Accordingly, the 3′-amino-oligonucleotides, the sequence of which was complementary to that of the glycoconjugates prepared, were first covalently immobilized on functionalized[37] 52-well glass slides.[38] Then, the glycocluster oligonucleotide derivatives **22** and **23**, the previously tested[12] galactosyl conjugates **24a–d**, and the additional galactosyl conjugate **25**, which had ten galactose residues, were hybridized onto the chip in order to compare their lectin-binding properties. Moreover, the trimannosyl conjugate **24e** was also immobilized as a negative control.

  

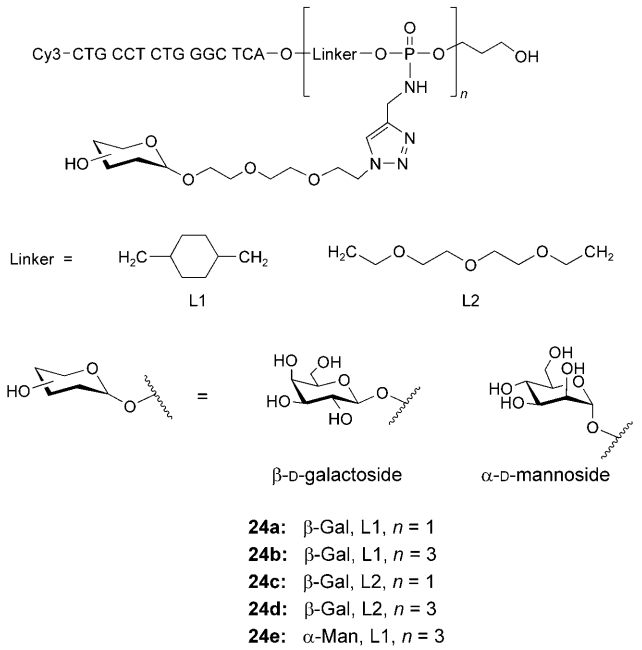


**24a:** β-Gal, L1, $n$ = 1
**24b:** β-Gal, L1, $n$ = 3
**24c:** β-Gal, L2, $n$ = 1
**24d:** β-Gal, L2, $n$ = 3
**24e:** α-Man, L1, $n$ = 3

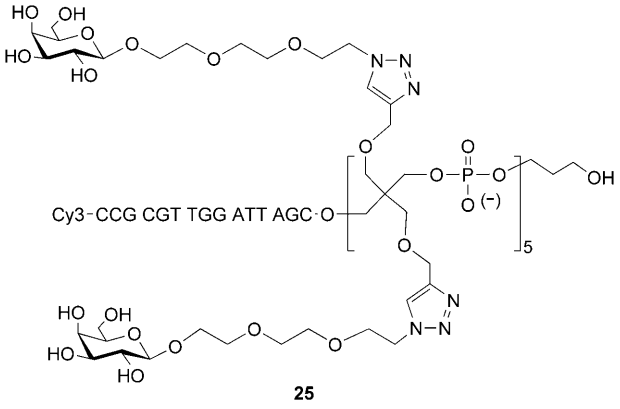


**25**

Glycoconjugate **25** was synthesized as described for the synthesis of **24a–e**, but in this case the alkyne functions were introduced by using a dialkyne phosphoramidite derivative.[11,34] Thus, starting from universal solid supported propane-1,3-diol, five dialkyne phosphoramidite derivatives were incorporated by phosphoramidite chemistry. The introduction of the ten galactose residues was performed by microwave-assisted[10] click chemistry, and then the oligonucleotide was synthesized and labeled with a Cy3 phosphoramidite. The desired glycoconjugate **25** was obtained after ammonia treatment and HPLC purification.

Scanning of the Cy3 fluorescence signal with a GenePix 4100A microarray scanner displayed a homogeneous hybridization of all conjugates, except for **25**, which included an oligonucleotide sequence that was different from that in the linear glycoconjugates **24a–e** (Figure 1). Two different Cy3 signals were observed for compound **24e** (each value was the mean of four spots on the same row). For one row, the signal intensity was similar to that observed for compounds **24a–d**, whereas for the other row it was approximately one third. Further experiments confirmed that compound **24e** hybridizes similarly to compounds **24a–d**.

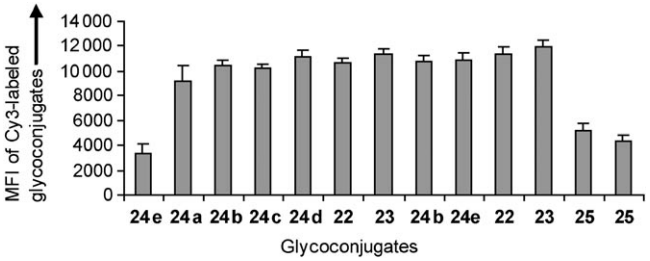


**Figure 1.** Mean fluorescence intensities (MFIs) at 532 nm (a.u.) of the Cy3-labeled glycoconjugates **22**–**25** after immobilization on the DNA chip.

We next studied the interactions of **22** and **23** with two different galactose-binding lectins: PA-IL[9] (*Pseudomonas aeruginosa* lectin) and RCA 120 (*Ricinus communis* agglutinin). PA-IL, which is the first lectin isolated from the Gram-negative bacterium *P. aeruginosa*,[39] features a narrow-specificity spectrum for molecules containing D-galactose. This protein is made up of four identical monomers, in which four calcium-dependent binding sites are located. After hybridization, the Alexa 647-labeled PA-IL was deposited in each well at 2.8 μM concentration, and after incubation and washing of the glass slide with Tween 20 in PBS solution (0.02%), the chip was scanned at 532 and 635 nm. The fluorescence signal of each conjugate was determined as the average mean fluorescence signal of four spots (Figure 2). The fluorescence image of Cy3 (Figure 2, left) showed that the glycoconjugates were still present after lectin incubation, whereas the fluorescence image of Alexa647 (Figure 2, right) was observed as a result of the binding of PA-IL. The selectivity of PA-IL for the corresponding galactose derivatives **24a–d** and **25** was demonstrated by the Alexa647 fluorescence signal at background level for the mannose-bearing glycoconjugate **24e** (Figure 3). The relative affinities of PA-IL towards the glycoconjugates can be directly monitored through the intensity of the lectin's fluorescence signal.

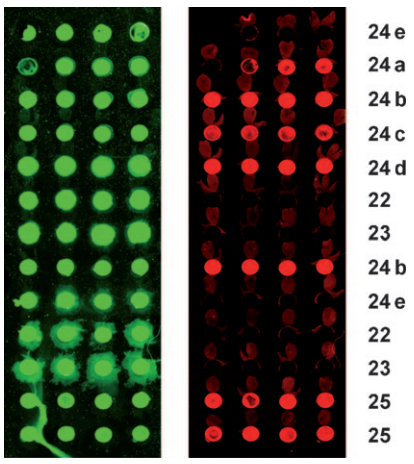


**Figure 2.** Fluorescence images recorded at 532 nm (left) and at 635 nm (right) after incubation of immobilized glycoconjugates **22**–**25** with Alexa 647-labeled PA-IL.

  

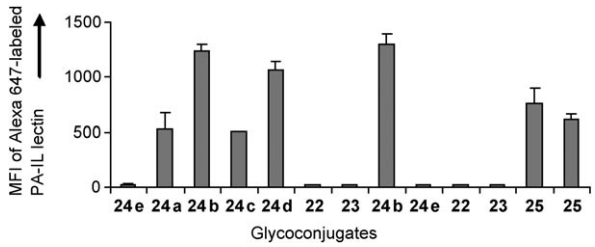


**Figure 3.** Mean fluorescence intensities (MFIs) at 635 nm (a.u.) of Alexa 647-labeled PA-IL after incubation with immobilized glycoconjugates **22**–**25**.

As previously observed with RCA 120,[12] glycoconjugates possessing three galactose residues (**24b** and **24d**) had better affinities towards PA-IL than those with only one residue (**24a** and **24c**), due to the expected cluster effect.[4,5] The nature of the linker (L1 and L2) between the galactose residues has little effect (**24b** vs. **24d**). Surprisingly, lower affinities were observed when the number of galactose moieties was increased. Thus, the deca-galactosyl conjugate (**25**) displayed a fluorescence signal weakened by a factor of two, whereas for both glycoconjugates **22** and **23**, as well as for the negative control **24e**, they were at background level, thus indicating that **22** and **23** did not have affinities towards PA-IL lectin (Figures 2 and 3).

Actually, it was expected that PA-IL should recognize **22** and **23** highly effectively, because they each featured a triazole ring β-D-linked to the galactose moiety, a molecular motif closely related to phenyl β-D-galactoside, the most potent known ligand for PA-IL. Two possible explanations for this finding can be advanced by considering either: 1) that steric hindrance might arise, or 2) that glycosylated calixarenes can sequester calcium ions, thus removing them from the binding site of the lectin. $^1$H NMR experiments were therefore carried out to evaluate the complexation abilities of glycoclusters **1** and **2** toward calcium(II) ions. The addition of anhydrous $Ca(ClO_4)_2$ to a solution of **1** in $CD_3OD$ led to an upfield shift (about 0.1 ppm) and a broadening of the signals due to the four aromatic protons resonating at $\delta = 6.47$–$6.40$ ppm and to two ($\delta = 2.1$ ppm) of the four upper-rim benzyl-type methylene groups. Downfield shifts of other signals in the central part of the spectrum ($\delta =$ 4.5–3.7 ppm) were also observed. In a similar way, after treatment of glycocluster **2** with $Ca(ClO_4)_2$, its $^1$H NMR spectrum (in $CD_3OD$) showed some changes. In particular, the signals of two ($\delta = 7.9$ ppm) of the four H-5 triazole atoms were slightly shifted downfield whereas the signals of four aromatic protons ($\delta = 6.3$ ppm) and four upper-rim aliphatic protons ($\delta =$ 2.0 ppm) underwent upfield shifts of about 0.1 ppm. To confirm the cation selectivity of the recognition process, the same experiments were repeated with replacement of $Ca(ClO_4)_2$ with anhydrous $NaClO_4$ in the $CD_3OD$ solutions. In this case, the spectra of **1** and **2** did not show any significant modification, suggesting that both glycoclusters can complex $Ca^{2+}$ ions when installed on the oligonucleotide chains and exposed to the lectin. This conclusion contrasted with the finding that no molecular recognition was detectable even on increasing the amounts of calcium ions in the tris/HCl buffer used instead of phosphate buffer. Therefore, we conclude that calcium sequestration cannot be taken as a causative effect for the lack of binding of **22** and **23** to PA-IL lectin. At this stage a convincing explanation for that observation is open to conjecture and may rather be related to steric hindrance.

These data showed that PA-IL recognizes glycoclusters with linear spatial structures more efficiently than it does those with antenna (**25**) and calixarene (**22** and **23**) structures. This result suggests that too close proximity between the galactose moieties has a negative effect on the recognition by PA-IL.

A similar affinity study was then performed with RCA 120, another lectin that recognizes galactose residues. RCA 120[40] is a heterodimeric protein with a $M_W$ of 60 kDa, made up of two S–S-linked chains A and B, the latter containing two carbohydrate-binding sites specific for galactose. Cy5-labeled RCA 120 was deposited in each well at 2 μM concentration and, after incubation and washing of the glass slide with Tween 20 in PBS solution (0.02%), it was scanned at 532 and 635 nm. The fluorescence image of Cy3 (Figure 4, left) confirmed that the glycoconjugates were still present after lectin incubation, whereas the fluorescence image of Cy5 (Figure 4, right) was observed as a result of the binding of RCA 120 with galactose residues.

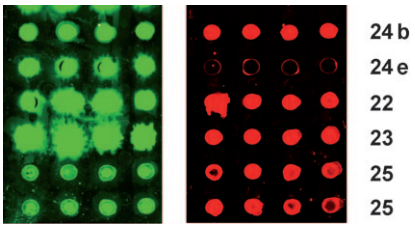


**Figure 4.** Fluorescence images recorded at 532 nm (left) and 635 nm (right) after incubation of immobilized glycoconjugates **22**, **23**, **24b**, **24e**, and **25** with Cy5-labeled RCA 120.

The fluorescence signal of each conjugate was determined as the average of the fluorescence signals of four spots. As would be expected, the Cy5 signal was at background level for the mannose-bearing glycoconjugate **24e**, highlighting the selectivity of RCA 120 for galactose (Figure 5). Interestingly, and in contrast with the data obtained with PA-IL, we found that all galactosylated glycoconjugates were able to bind RCA 120. Therefore, in this case, the use of the unnatural calixarene scaffold and triazole linker did not prevent the molecular recognition of the sugar ligand by the lectin. The glycoconjugate **23**, bearing eight galactose residues, displayed an affinity similar to that observed for **24b**, the most active compound, featuring only three galactose moieties. The ratio of the intensities of the Cy5 signals for **23** and **22** was in the 1.2–2 range (from independent experiments), whereas the ratio of the galactose residues linked to these glycoconjugates was 2. Surprisingly, RCA 120 bound with a lower affinity to compound **25**, bearing ten residues in an antenna-based spatial arrangement. These results indicate that the three-dimensional orientation of the sugar units is more important than their number. In fact **24b**, bearing three galactose residues in a linear arrangement, was

  

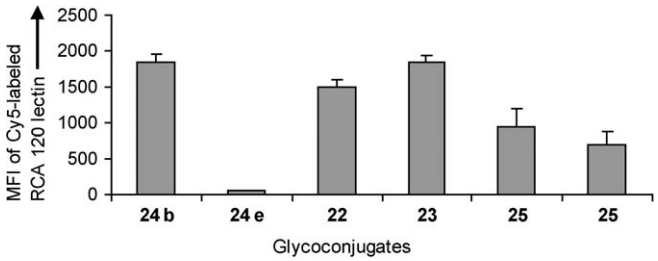


**Figure 5.** Mean fluorescence intensities (MFIs) at 635 nm (a.u.) of Cy5-labeled RCA 120 after incubation with immobilized glycoconjugates **22**, **23**, **24 b**, **24 e**, and **25**.

the most potent ligand out of the seven glycoconjugates tested in this study.

In order to provide a quantitative analysis of the binding affinities between lectin RCA 120 and glycoconjugates **22** and **23**, the corresponding $IC_{50}$ values were measured as previously reported[41] and compared with the $IC_{50}$ values determined for **24 a** and **24 b**.[13] We determined $IC_{50}$ values as the concentration of lactose required for the removal of 50% of RCA 120 bound to the immobilized glycoconjugates. The glycoconjugates **22** or **23** were immobilized by hybridization at the bottoms of the microwells and further incubated with mixtures of Cy5-labeled RCA 120 (2 μM) containing increasing concentrations of lactose (0.05 μM to 30 mM). Fluorescence images at 532 and 635 nm were then obtained after washing of the glass slides to remove the unbound lectins (Figure 6). Each experimental point is an average value of four spots.

The Cy5 fluorescence intensities were tabulated against logarithmic lactose concentrations (Figure 7).

The $IC_{50}$ values for the monogalactose **24 a**,[13] the trigalactose **24 b**,[13] the tetragalactose **22**, and the octagalactose **23** glycoconjugates are displayed in Table 1.

As would be expected, we found that the affinity of RCA 120 increased along with the number of galactose residues, due to higher local galactose concentrations. $IC_{50}$ measurements confirmed that RCA 120 had affinities for compounds **24 b** and **23** in the same range. Moreover, the $IC_{50}$ value for **23** was 2.7 times higher than that for **22**, leading to an affinity per residue increased by a factor of 1.3, whereas values in the 1.2–2 range were obtained when analyzed by fluorescence of Cy5 (Figure 5). Therefore, as already reported,[5] the measured cluster effect depends on the assay conditions.

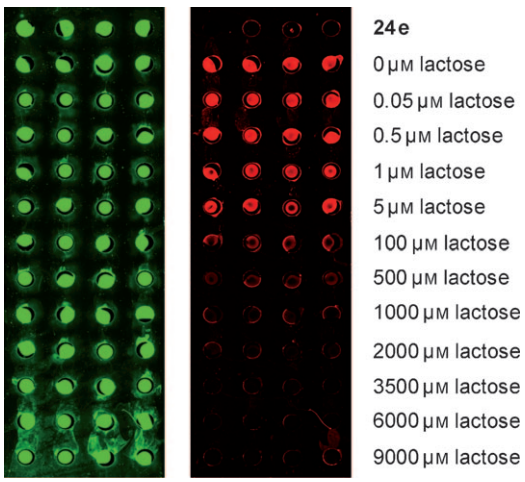


**Figure 6.** Typical fluorescence images recorded at 532 nm (left) and 635 nm (right) after incubation of **22** or **23** with Cy5-labeled RCA 120 and increasing concentrations of lactose.

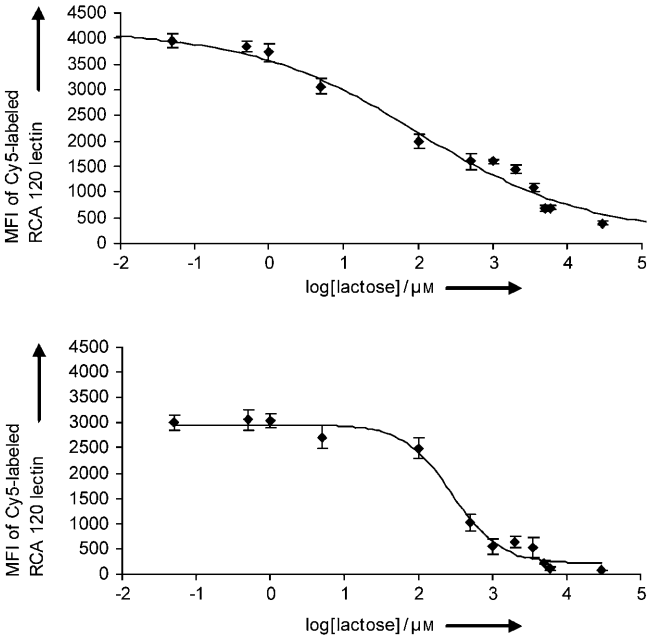


**Figure 7.** Competitive curves of Cy5-RCA 120 with **22** (top) and **23** (bottom) immobilized on DNA chips in the presence of increasing concentrations of lactose. Mean fluorescence intensities (MFIs) at 635 nm (a.u.).

**Table 1.** $IC_{50}$ values for the binding between glycoconjugates and RCA 120.

| Glycoconjugate | Valency | $IC_{50}$ [μM] | Relative potency[a] | Potency per galactose residue[b] |
|---|---|---|---|---|
| **24 a** | 1 | 5.6 ± 2.8[13] | 1 | 1 |
| **24 b** | 3 | 385 ± 45[13] | 69 | 23 |
| **22** | 4 | 114 ± 14 | 20 | 5 |
| **23** | 8 | 305 ± 22 | 54 | 7 |

[a] Ratio of multivalent glycoconjugates to monovalent glycoconjugate **24 a** $IC_{50}$ values. [b] Ratio of relative potency to the number of galactose residues.

## Conclusions

This study has shown that each class of galactose cluster (linear, calixarene, and antenna) is recognized with different affinities by PA-IL and RCA 120 lectins. Our results showed that the spatial arrangement is more important than the number of galactose residues, because the linear trivalent clusters (**24 b** and **24 d**) were better able to bind lectins than antenna (**25**) and calixarene (**22** and **23**) ones with 10, four, and eight galactose moieties, respectively. Furthermore, we showed that PA-IL

  

is more selective than RCA 120, because galactosyl-calixarene derivatives **22** and **23** were not recognized by PA-IL.

The importance of the spatial arrangement of the glycoside residues in the lectin recognition process has been assessed for the asialoglycoprotein receptor.[12,42,43] It was shown that the trigalactose cluster with the largest distance between the sugar residues presents the optimal recognition.[39,42] The recognition study was performed by direct fluorescence scanning and by the determination of the $IC_{50}$ values, with both techniques leading to similar results.

The carbohydrate microarray used in this study required only minute amounts of material. The synthesis of the glycoconjugates could therefore be performed on a fairly small scale, but the miniaturization through the microarray technology provided the biological data for a complete study.

## Experimental Section

**Synthesis of 5′-Cy3-oligonucleotides with 3′-mono- or 3′-dialkyne functions**: The oligonucleotides were synthesized on a DNA synthesizer (ABI 394) by standard phosphoramidite chemistry from the starting monoalkyne **16** or dialkyne **17** solid supports (synthesized as previously described[36]). Detritylation was performed with DCA in $CH_2Cl_2$ (3%) for 35 s for the dimethoxytrityl groups and for 60 s for the monomethoxytrityl group (Cy3). For the coupling step, benzylmercaptotetrazole (0.3 M in anhydrous $CH_3CN$) was used as activator, and commercially available phosphoramidites (A, T, C, G, Cy3; 0.075 M in anhydrous $CH_3CN$) were introduced with a 20 s coupling time. The capping step was performed with acetic anhydride by use of a commercial solution (Cap A: $Ac_2O$/pyridine/THF 10:10:80 and Cap B: 10% *N*-methylimidazole in THF) for 15 s. Oxidation was performed with a commercially available solution of iodine (0.1 M $I_2$, THF/pyridine/water 90:5:5) for 13 s.

**Synthesis of 5′-Cy3-CCG CGT TGG ATT AGC (PePO galactosyl$_2$)$_5$ propanol (25)**: Starting from the propane-1,3-diol-bound solid support, five 3-(4,4′-dimethoxytrityloxy)-2,2-bis(propargyloxymethyl)-propyl (2-cyanoethyl *N*,*N*-diisopropyl)-phosphoramidite[11] units were coupled according to the phosphoramidite elongation cycle (see above), and this was followed by the first three nucleotides. Solid-supported DMTr-$A^{bz}G^{ibu}C^{bz}$ decaalkyne derivative (0.6 μmol) was transferred into a microwave vial, and 1-azido-3,6-dioxaoct-8-yl 2,3,4,6-tetra-*O*-acetyl-β-D-galactopyranoside[12,44] (30 μmol, 15.2 mg, in 100 μL of methanol), $CuSO_4$ (1.2 μmol, 6 μL of 200 mM water solution) and sodium ascorbate (6 μmol, 24 μL of 250 mM water solution) were added. The sealed vial was irradiated with microwaves for 20 min at 60 °C with magnetic stirring. After filtration, washing with methanol/water and dry acetonitrile, and drying in a desiccator, the beads were transferred to a DNA column and the sequence was completed on the DNA synthesizer with a Cy3 at the 5′ end. After deprotection and HPLC purification the pure **25** was characterized by MALDI-TOF MS; *m/z* calcd for $C_{353}H_{531}N_{87}O_{208}P_{21}$: 9972.02 $[M-H]^-$; found: 9971.03.

**General procedure for deprotection**: The beads were treated with concentrated aqueous ammonia (~1 mL) at 55 °C for 6 h, and the supernatant was then withdrawn and concentrated to dryness. The residue was dissolved in water for subsequent analyses.

**Cu$^I$-catalyzed cycloadditions for mono- and dicalix[4]arene oligonucleotide conjugates 22 and 23**: Compound **1** (4 equiv, 100 μL of a 0.02 M solution in water), $CuSO_4$ (5 equiv, 2.5 μmol, 13 μL of a 0.2 M solution in $H_2O$), freshly prepared sodium ascorbate (25 equiv, 12.5 μmol, 64 μL of a 0.2 M solution in $H_2O$), and water (300 μL) were added to monoalkyne oligonucleotide **20** (0.5 μmol). The mixture was heated at 60 °C for 1 h in a sealed tube by use of a microwave synthesizer Initiator from Biotage (temperature monitored with an internal infrared probe). Saturated aqueous EDTA solution (500 μL) was then added to the mixture, and the resulting solution was desalted on NAP10. The crude product was purified by reversed-phase preparative HPLC to yield pure compound **22** (111 nmol), determined by spectrophotometry at 550 nm ($\varepsilon_{(Cy3)} = 150\,000$). $t_R$ (HPLC) = 15.42 min; MALDI-TOF MS: *m/z* calcd for $C_{264}H_{345}N_{68}O_{124}P_{16}$: 6950.62 $[M-H]^-$; found: 6949.63.

The synthesis of conjugate **23** (70 nmol) was performed as described above with the use of **21** and 6 equiv of **2**. $t_R$ (HPLC) = 17.18 min; MALDI-TOF MS: *m/z* calcd for $C_{366}H_{490}N_{85}O_{157}P_{16}$: 9087.98 $[M-H]^-$; found: 9090.22.

**Fabrication of microarrays**[12]

*Silanization of the glass slides*: Borosilicate glass slides (Schott) containing 52 microreactors[38] (2 mm diameter, 65–100 μm deep) were functionalized by the protocol developed by Dugas et al.[37] In brief, after piranha treatment, the slides were heated under dry nitrogen at 150 °C for 2 h. Next, dry pentane (250 mL) and *tert*-butyl-11-(dimethylamino)silylundecanoate (300 μL) were added at room temperature. After 20 min of incubation, the pentane was evaporated and the slides were heated at 150 °C overnight. Functionalized slides were obtained after washing in THF and rinsing in water. Deprotection of the ester function was performed with formic acid (7 h at room temperature). *N*-Hydroxysuccinimide (0.1 M) and diisopropylcarbodiimide (0.1 M) in dry THF were used for the activation of the acid functions.

*Immobilization of DNA strands*: 3′-Amino-modified oligonucleotides were purchased from Eurogentec. Sequence 1 (S1: 5′-GTG AGC CCA GAG GCA GGG-$(CH_2)_7$-$NH_2$), sequence 2 (S2: 5′-GCT AAT CCA ACG CGG GCC AAT CCT T-$(CH_2)_7$-$NH_2$) and sequence 3 (negative control, S3: 5′-ATG CCC TCT TTG ATA TT-$(CH_2)_7$-$NH_2$) were used. The desired sequence (1 μL of a 25 μM solution in 10×PBS at pH 8.5) was deposited at the bottom of the corresponding well. The coupling reaction was performed overnight at room temperature. Water was then allowed slowly to evaporate. The slides were washed with SDS (0.1%) at 70 °C for 30 min and rinsed with deionized water.

*Blocking*: After immobilization, all slides were blocked with bovine serum albumin (BSA). Blocking was performed with a BSA solution (4%) in 1×PBS (pH 7.4), at room temperature for 2 h. The glass slides were then washed in 1×PBS (pH 7.4)/Tween 20 (0.05%) 3× 3 min followed by 1×PBS (pH 7.4) two to three times, rinsed with deionized water, and dried by centrifugation.

*Hybridization of the glycoconjugates on DNA array*: Glycoconjugates bearing a DNA tag were hybridized with a solution (1 μL) at the desired concentrations (5×SSC, 0.1% SDS), placed at the bottom of the corresponding well, and allowed to hybridize overnight at room temperature in a $H_2O$-vapor-saturated chamber. The slides were washed in 2×SSC, SDS (0.1%) at 51 °C for 1 min, followed by 2×SSC at room temperature for an additional 5 min, and were then rinsed with deionized water and dried by centrifugation.

**Probing microarrays**

*Cy5 labeling of RCA 120 lectin*: RCA 120 (Sigma) was labeled by use of an Amersham Biosciences Cy5 Ab Labeling Kit according to the manufacturer's protocol. Protein concentration and the dye/protein ratio were estimated by optical density (nanodrop), with reading

  

of the absorbance at 280 and 650 nm. Lectin concentration was estimated to be 4 μM, bearing an average of four dyes per protein.

Labeling of PA-IL lectin (a gift from Dr. Anne Imberty, CERMAV) with Alexa647 was performed by use of the microscale labeling kit from Invitrogen. Protein concentration was estimated according to the manufacturer's protocol by reading of the absorbance at 280 and 650 nm. The final lectin concentration was estimated at 28 μM with a degree of labeling of 0.4.

The labeled lectin was diluted in 1×PBS (pH 7.4), $CaCl_2$ (final concentration 5 μM), and 20% BSA (final concentration 2%) to the desired concentration. For $IC_{50}$ experiments, lactose was added to the solutions at different final concentrations. Each solution (1 μL) was placed at the bottom of each well and incubated at 37 °C in a $H_2O$-vapor-saturated chamber for 2 h. The slides were then washed in 1×PBS (pH 7.4)/Tween 20 (0.02%) for 10 min, dried by centrifugation, and scanned.

*Fluorescence scanning*: Fluorescent scanning was performed with a Microarray scanner, GenePix 4100A and software package (Axon Instruments; $\lambda_{ex}$ 532/635 nm and $\lambda_{em}$ 575/670 nm). The fluorescence signal of each conjugate was determined as the average of the mean fluorescence signals of four spots.

## Acknowledgements

*This work was financially supported by the CNRS interdisciplinary program "Interface Physique Chimie Biologie: soutien à la prise de risque". ANR-08-BLAN-0114-01 and Lyon Biopole are also acknowledged for financial support. The Chinese Scientific Council is gratefully acknowledged for a scholarship to J.Z. G.P. thanks the CNRS and the Région Languedoc–Roussillon for the award of a research studentship. NanoLyon is acknowledged for technical support. We thank Anne Imberty for a generous gift of PA-IL lectin. HRMS analyses were performed by Dr. A. Chambery (II Università di Napoli, Caserta, Italy). F.M. is a member of INSERM.*

**Keywords:** calixarenes · click chemistry · glycoarrays · glycoclusters · multivalency

[1] N. Firon, S. Ashkenazi, D. Mirelman, I. Ofek, N. Sharon, *Infect. Immun.* **1987**, *55*, 472–476.
[2] R. Roy, M.-G. Baek, *Rev. Mol. Biotechnol.* **2002**, *90*, 291–309.
[3] R. T. Lee, Y. C. Lee in *Enhanced Biochemical Affinities of Multivalent Neoglycoconjugates* (Eds.: R. T. Lee, Y. C. Lee), Academic Press, San Diego, **1994**, pp. 23–50.
[4] Y. C. Lee, R. T. Lee, *Acc. Chem. Res.* **1995**, *28*, 321–327.
[5] J. J. Lundquist, E. J. Toone, *Chem. Rev.* **2002**, *102*, 555–576.
[6] A. Salminen, V. Loimaranta, J. A. F. Joosten, A. S. Khan, J. Hacker, R. J. Pieters, J. Finne, *J. Antimicrob. Chemother.* **2007**, *60*, 495–501.
[7] a) K. Matsuura, M. Hibino, T. Ikeda, Y. Yamada, K. Kobayashi, *Chem. Eur. J.* **2004**, *10*, 352–359; b) T. Ohta, N. Miura, N. Fujitani, F. Nakajima, K. Niikura, R. Sadamoto, C.-T. Guo, T. Suzuki, Y. Suzuki, K. Monde, S.-I. Nishimura, *Angew. Chem.* **2003**, *115*, 5344–5347; *Angew. Chem. Int. Ed.* **2003**, *42*, 5186–5189; c) G. D. Glick, P. L. Toogood, D. C. Wiley, J. J. Skehel, J. R. Knowles, *J. Biol. Chem.* **1991**, *266*, 23660–23669.
[8] S. André, F. Sansone, H. Kaltner, A. Casnati, J. Kopitz, H.-J. Gabius, R. Ungaro, *ChemBioChem* **2008**, *9*, 1649–1661.
[9] A. Imberty, M. Wimmerová, E. P. Mitchell, N. Gilboa-Garber, *Microbes Infect.* **2004**, *6*, 221–228.
[10] C. Bouillon, A. Meyer, S. Vidal, A. Jochum, Y. Chevolot, J. P. Cloarec, J. P. Praly, J. J. Vasseur, F. Morvan, *J. Org. Chem.* **2006**, *71*, 4700–4702.
[11] F. Morvan, A. Meyer, A. Jochum, C. Sabin, Y. Chevolot, A. Imberty, J. P. Praly, J. J. Vasseur, E. Souteyrand, S. Vidal, *Bioconjugate Chem.* **2007**, *18*, 1637–1643.
[12] Y. Chevolot, C. Bouillon, S. Vidal, F. Morvan, A. Meyer, J. P. Cloarec, A. Jochum, J. P. Praly, J. J. Vasseur, E. Souteyrand, *Angew. Chem.* **2007**, *119*, 2450–2454; *Angew. Chem. Int. Ed.* **2007**, *46*, 2398–2402.
[13] J. Zhang, G. Pourceau, A. Meyer, S. Vidal, J. P. Praly, E. Souteyrand, J. J. Vasseur, F. Morvan, Y. Chevolot, *Biosens. Bioelectron.* **2009**, *24*, 2515–2521.
[14] a) V. V. Rostovtsev, L. G. Green, V. V. Fokin, K. B. Sharpless, *Angew. Chem.* **2002**, *114*, 2708–2711; *Angew. Chem. Int. Ed.* **2002**, *41*, 2596–2599; b) C. W. Tornøe, C. Christensen, M. Meldal, *J. Org. Chem.* **2002**, *67*, 3057–3064; c) V. D. Bock, H. Hiemstra, J. H. van Maarseveen, *Eur. J. Org. Chem.* **2006**, 51–58; d) S. Dedola, S. A. Nepogodiev, R. A. Field, *Org. Biomol. Chem.* **2007**, *5*, 1006–1017; e) A. Dondoni, *Chem. Asian J.* **2007**, *2*, 700–708; f) J.-F. Lutz, *Angew. Chem.* **2007**, *119*, 1036–1043; *Angew. Chem. Int. Ed.* **2007**, *46*, 1018–1025; g) J. E. Moses, A. D. Moorhouse, *Chem. Soc. Rev.* **2007**, *36*, 1249–1262; h) P. Wu, V. V. Fokin, *Aldrichimica Acta* **2007**, *40*, 7–17; i) M. Meldal, C. W. Tornøe, *Chem. Rev.* **2008**, *108*, 2952–3015.
[15] Selected reviews: a) C. D. Gutsche, *Aldrichimica Acta* **1995**, *28*, 3–9; b) V. Böhmer, *Angew. Chem.* **1995**, *107*, 785–818; *Angew. Chem. Int. Ed. Engl.* **1995**, *34*, 713–745; c) V. Böhmer, *Liebigs Ann.* **1997**, 2019–2030; d) A. Ikeda, S. Shinkai, *Chem. Rev.* **1997**, *97*, 1713–1734.
[16] C. D. Gutsche, J. A. Levine, P. K. Sujeeth, *J. Org. Chem.* **1985**, *50*, 5802–5806.
[17] a) J.-D. van Loon, A. Arduini, L. Coppi, W. Verboom, A. Pochini, R. Ungaro, S. Harkema, D. N. Renhoudt, *J. Org. Chem.* **1990**, *55*, 5639–5646; b) A. Arduini, M. Fabbri, M. Mantovani, L. Mirone, A. Pochini, A. Secchi, R. Ungaro, *J. Org. Chem.* **1995**, *60*, 1454–1457.
[18] K. Iwamoto, K. Araki, S. Shinkai, *J. Org. Chem.* **1991**, *56*, 4955–4962.
[19] Z.-C. Ho, M.-C. Ku, C.-M. Shu, L.-G. Lin, *Tetrahedron* **1996**, *52*, 13189–13200.
[20] C.-M. Shu, W.-S. Chung, S.-H. Wu, Z.-C. Ho, L.-G. Lin, *J. Org. Chem.* **1999**, *64*, 2673–2679.
[21] a) C. D. Gutsche, B. Dhawam, J. A. Levine, K. Hyun, L. J. Bauer, *Tetrahedron* **1983**, *39*, 409–426; b) K. Iwamoto, K. Araki, S. Shinkai, *Tetrahedron* **1991**, *47*, 4325–4342; c) A. Dondoni, C. Ghiglione, A. Marra, M. Scoponi, *J. Org. Chem.* **1998**, *63*, 9535–9539.
[22] a) A. Marra, M.-C. Scherrmann, A. Dondoni, A. Casnati, P. Minari, R. Ungaro, *Angew. Chem.* **1994**, *106*, 2533–2535; *Angew. Chem. Int. Ed. Engl.* **1994**, *33*, 2479–2481; b) A. Dondoni, A. Marra, M.-C. Scherrmann, A. Casnati, F. Sansone, R. Ungaro, *Chem. Eur. J.* **1997**, *3*, 1774–1782.
[23] a) A. Marra, A. Dondoni, F. Sansone, *J. Org. Chem.* **1996**, *61*, 5155–5158; b) A. Dondoni, M. Kleban, X. Hu, A. Marra, H. D. Banks, *J. Org. Chem.* **2002**, *67*, 4722–4733; c) A. Dondoni, A. Marra, *Tetrahedron* **2007**, *63*, 6339–6345.
[24] a) A. Dondoni, A. Marra, *J. Org. Chem.* **2006**, *71*, 7546–7557; b) A. Marra, L. Moni, D. Pazzi, A. Corallini, D. Bridi, A. Dondoni, *Org. Biomol. Chem.* **2008**, *6*, 1396–1409.
[25] A. Vecchi, B. Melai, A. Marra, C. Chiappe, A. Dondoni, *J. Org. Chem.* **2008**, *73*, 6437–6440.
[26] H. M. Chawla, N. Pant, B. Srivastava, *Tetrahedron Lett.* **2005**, *46*, 7259–7262.
[27] L. C. Groenen, B. H. M. Ruël, A. Casnati, W. Verboom, A. Pochini, R. Ungaro, D. N. Reinhoudt, *Tetrahedron* **1991**, *47*, 8379–8384.
[28] F. Santoyo-González, A. Torres-Pinedo, A. Sanchéz-Ortega, *J. Org. Chem.* **2000**, *65*, 4409–4414.
[29] For two-step approaches to calix[4]arene derivatives monoalkylated at the lower rim see: a) A. Casnati, A. Arduini, E. Ghidini, A. Pochini, R. Ungaro, *Tetrahedron* **1991**, *47*, 2221–2228; b) S. Taghvaei-Ganjali, A. Modjallal, *Acta Chim. Slov.* **2001**, *48*, 427–430.
[30] T. Lowary, M. Meldal, A. Helmboldt, A. Vasella, K. Bock, *J. Org. Chem.* **1998**, *63*, 9657–9668.
[31] E. D. Goddard-Borger, R. V. Stick, *Org. Lett.* **2007**, *9*, 3797–3800.
[32] R. K. Castellano, D. M. Rudkevich, J. Rebek, *Proc. Natl. Acad. Sci. USA* **1997**, *94*, 7132–7137.
[33] S. L. Beaucage, M. H. Caruthers, *Tetrahedron Lett.* **1981**, *22*, 1859–1862.
[34] G. Pourceau, A. Meyer, J. J. Vasseur, F. Morvan, *J. Org. Chem.* **2008**, *73*, 6014–6017.
[35] J. Lietard, A. Meyer, J. J. Vasseur, F. Morvan, *J. Org. Chem.* **2008**, *73*, 191–200.

  

[36] R. Kumar, A. El-Sagheer, J. Tumpane, P. Lincoln, L. M. Wilhelmsson, T. Brown, *J. Am. Chem. Soc.* **2007**, *129*, 6859–6864.
[37] V. Dugas, G. Depret, B. Chevalier, X. Nesme, E. Souteyrand, *Sens. Actuators B* **2004**, *101*, 112–121.
[38] R. Mazurczyk, G. E. Khoury, V. Dugas, B. Hannes, E. Laurenceau, M. Cabrera, S. Krawczyk, E. Souteyrand, J. P. Cloarec, Y. Chevolot, *Sens. Actuators B* **2008**, *128*, 552–559.
[39] A. Imberty, M. Wimmerová, C. Sabin, E. P. Mitchell in *Protein–Carbohydrate Interactions in Infectious Diseases* (Ed.: C. Bewley), RSC, Cambridge, **2006**, pp. 30–45.
[40] H. Lis, N. Sharon, *Chem. Rev.* **1998**, *98*, 637–674.
[41] S. Park, M. R. Lee, S. J. Pyo, I. Shin, *J. Am. Chem. Soc.* **2004**, *126*, 4812–4819.
[42] E. A. L. Biessen, D. M. Beuting, H. C. P. F. Roelen, G. A. van de Marel, J. H. van Boom, T. J. C. van Berkel, *J. Med. Chem.* **1995**, *38*, 1538–1546.
[43] Y. C. Lee, R. R. Townsend, M. R. Hardy, J. Lönngren, J. Arnarp, M. Haraldsson, H. Lönn, *J. Biol. Chem.* **1983**, *258*, 199–202.
[44] Z. Szurmai, L. Szabó, A. Lipták, *Acta Chim. Hung.* **1989**, *126*, 259–269.

Received: January 16, 2009
Published online on April 29, 2009

  